A functional AMPA receptor–calcium channel complex in the postsynaptic membrane

Myoung-Goo Kang*, Chien-Chang Chen*, Minoru Wakamori†, Yuji Hara†, Yasuo Mori†, and Kevin P. Campbell*‡

*Howard Hughes Medical Institute and Departments of Physiology and Biophysics, Internal Medicine, and Neurology, University of Iowa Roy J. and Lucille A. Carver College of Medicine, Iowa City, IA 52242; and †Laboratory of Molecular Biology, Department of Synthetic Chemistry and Biological Chemistry, Graduate School of Engineering, Kyoto University, Kyoto 615-8510, Japan

Contributed by Kevin P. Campbell, February 16, 2006

Ca^{2+} channels play critical roles in the regulation of synaptic activity. In contrast to the well established function of voltage-activated Ca^{2+} channels in the presynaptic membrane for neurotransmitter release, some studies are just beginning to elucidate the functions of the Ca^{2+} channels in the postsynaptic membrane. In this study, we demonstrated the functional association of α-amino-3-hydroxy-5-methyl-4-isoxazolepropionate (AMPA) receptors with the neuronal Ca^{2+} channels. A series of biochemical studies showed the specific association of $Ca_v2.1$ (α_{1A}-class) and $Ca_v2.2$ (α_{1B}-class) with AMPA receptors in the postsynaptic membrane. Our electrophysiological and Ca^{2+} imaging analyses of recombinant $Ca_v2.1$ and AMPA receptors also showed functional coupling of the two channels. Considering the critical roles of postsynaptic intracellular concentration of Ca^{2+} ($[Ca^{2+}]_i$) increase and AMPA receptor trafficking for long-term potentiation (LTP) and long-term depression (LTD), the functional association of Ca^{2+} channels with the AMPA receptors may provide new insights into the mechanism of synaptic plasticity.

voltage-activated Ca^{2+} channel | stargazin | glutamate receptor | synaptic plasticity | postsynaptic density

Neurotransmitter-mediated communication between a presynaptic and a postsynaptic membrane is a fundamental neurophysiological phenomenon. The precise organization and dynamic change of presynaptic and postsynaptic protein components underlies the physiological regulation of synaptic efficacy. The study of the organization and dynamics of synaptic proteins is the key to our understanding of synaptic plasticity, neuronal development, and some neurological disorders.

The α-amino-3-hydroxy-5-methyl-4-isoxazolepropionate (AMPA) receptor is one of the major types of glutamate receptors (GluRs) mediating neurotransmission in the excitatory postsynaptic membrane. Activity-dependent trafficking of AMPA receptors in and out of the postsynaptic membrane is one of the key mechanisms for synaptic plasticity such as long-term potentiation (LTP) and long-term depression. Although recent studies have identified several postsynaptic proteins that interact with the AMPA receptor C terminus and are potentially involved in AMPA receptor trafficking, the precise mechanism for the modulation of AMPA receptors trafficking in the postsynaptic membrane is still not clear (1).

Voltage-activated Ca^{2+} channels function in many fundamental physiological processes, including neurotransmission, muscle contraction, intracellular signaling, hormone secretion, and development. The function of voltage-activated Ca^{2+} channels (called Ca^{2+} channels or Ca_v hereafter) for neurotransmission in the presynaptic membrane has been intensively studied because the Ca^{2+} channel is a key player in the coupling of electric and chemical signals in presynapses. In addition to the presynaptic function, postsynaptic function of Ca^{2+} channels is beginning to be revealed through recent biophysical studies. Induction of hippocampal mossy fiber LTP by brief high-frequency stimulation (B-HFS) requires an influx of Ca^{2+} through voltage-activated Ca^{2+} channels at the postsynapse (2). Brain-derived neurotrophic factor (BDNF)-mediated LTP in hippocampal neurons requires activation of postsynaptic voltage-activated Ca^{2+} channels (3).

It is known that the neuronal high-voltage-activated Ca^{2+} channel consists of at least three subunits: a main subunit, α_1, and two auxiliary subunits, β and $\alpha_2\delta$ (4). In addition, the association of the γ subunits (γ_2 and γ_3) with neuronal Ca^{2+} channels has recently been established (5, 6), which is similar to the association of γ_1 subunit with skeletal Ca^{2+} channels (7). Interestingly, a role of the γ_2 subunits (stargazin) in the trafficking/clustering of AMPA receptors has been reported (8–11). Stargazin functions as a chaperon protein for proper folding and surface expression of AMPA receptors. Stargazin also involves in the synaptic targeting of AMPA receptors through its interaction with PSD95, a scaffolding protein enriched in postsynaptic density (PSD). In addition, a recent study showed involvement of stargazin in cell aggregation (12). Taken together, these studies suggest the intriguing possibility that the γ_2 subunit has more than one function in the brain.

In this article, we examined the association of AMPA receptors with neuronal Ca^{2+} channels through biochemical, electrophysiological, and Ca^{2+}-imaging analyses. Our results show that native neuronal Ca^{2+} channels can form a large complex with postsynaptic proteins in the postsynaptic membrane and that this association could change some biophysical properties of these Ca^{2+} channels and AMPA receptors.

Results

To study the composition of voltage-activated Ca^{2+} channels complex, the Ca^{2+} channel complexes were enriched from rabbit brain or skeletal muscle through microsome preparation, KCl wash, solubilization, wheat germ agglutinin (WGA) chromatography, and sucrose gradient fractionation as described in *Methods*. Western blot analysis of sucrose gradient fractions with anti-Ca^{2+} channel subunit antibodies showed cosedimentation of all subunits in the same fractions in each preparation, indicating that the integrity of Ca^{2+} channels was not disrupted during the partial purification process (Fig. 1 *A* and *B*). Comparison of brain and skeletal muscle Ca^{2+} channel complexes shows that the brain complex is larger in size than the skeletal muscle complex (Fig. 1 *A* and *B*). Likewise, when brain Ca^{2+} channel complexes were enriched through alternative heparin chromatography instead of WGA chromatography, we observed a difference in the size of the Ca^{2+} channel complex (Fig. 1 *A* and *C*), which is very similar to the difference in size between the brain and skeletal muscle Ca^{2+} channel complexes (Fig. 1 *A* and *B*). The size of Ca^{2+} channel complexes in sucrose gradient after heparin chromatography is very similar to that of completely

Conflict of interest statement: No conflicts declared.

Abbreviations: AMPA, α-amino-3-hydroxy-5-methyl-4-isoxazolepropionate; PSD, postsynaptic density; WGA, wheat germ agglutinin; HEK, human embryonic kidney; GluR, glutamate receptor.

‡To whom correspondence should be addressed. E-mail: kevin-campbell@uiowa.edu.

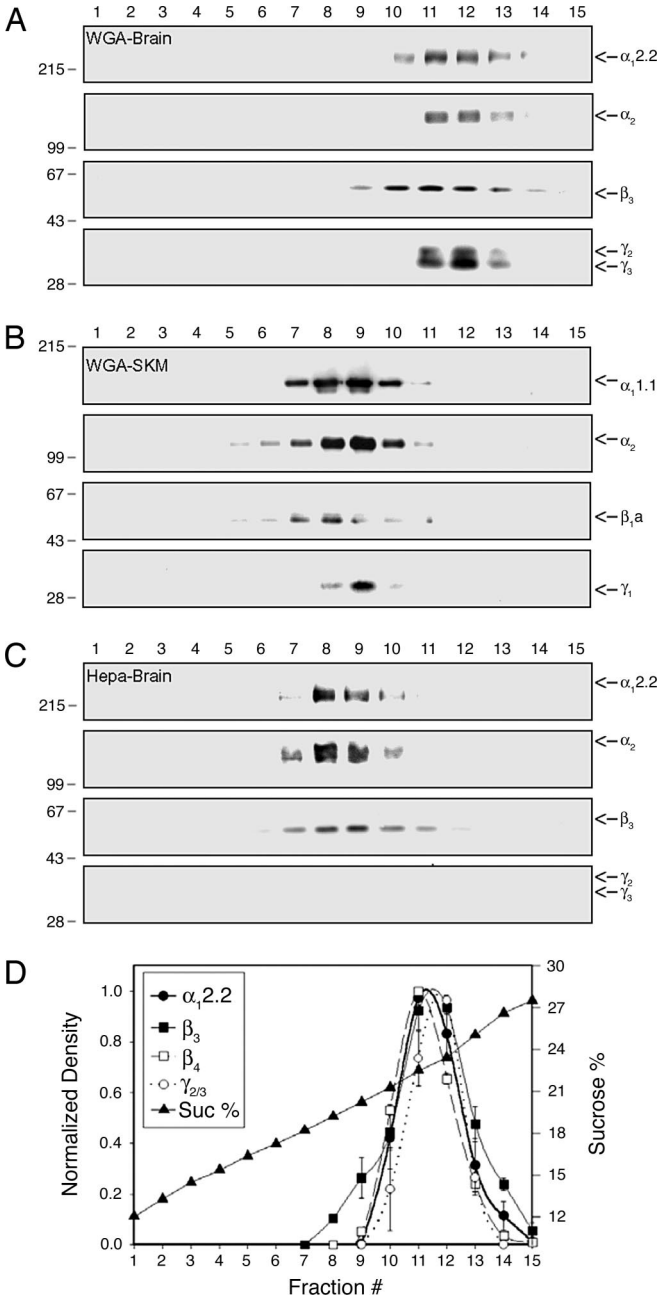

Fig. 1. Comparison of the Ca^{2+} channel complex partially purified from different tissues or through different methods. Sucrose gradient fractionation of Ca^{2+} channel complexes and subsequent immunoblotting for Ca^{2+} channel subunits demonstrate that the size of partially purified Ca^{2+} channel complexes differs depending on tissue and purification method. (*A*) Sucrose gradient fractionation of WGA-bound Ca^{2+} channel complex from rabbit brains. (*B*) Sucrose gradient fractionation of WGA-bound Ca^{2+} channel complex from rabbit skeletal muscles (SKM). (*C*) Sucrose gradient fractionation of heparin-bound Ca^{2+} channel complex from rabbit brains. The numbers at the top indicate the fraction of the sucrose gradient from top to bottom. Molecular mass standards ($\times 10^{-3}$) are indicated on the left side of the panels. (*D*) Densitometry of Ca^{2+} channel subunits from Western blots of sucrose gradient fractions of WGA-bound Ca^{2+} channel complex. Fraction #, fraction number of sucrose gradient; Sucrose %, percentage of sucrose.

purified N-type Ca^{2+} channel complexes in a previous study (4). This result suggests that brain Ca^{2+} channel complexes partially purified through WGA chromatography are associated with some additional neuronal proteins that do not exist in skeletal muscle and that these proteins are dissociated during the process of heparin chromatography. Interestingly, the γ_2 and γ_3 subunits are part of the neuronal proteins dissociated during the process of heparin chromatography (Fig. 1*C*). In addition, as a statistical analysis of the cosedimentation data, we plotted the normalized density of each protein as a function of sucrose gradient fraction number and sucrose percentage using data from five or six Western blot analyses of independent partial purification through WGA chromatography. As expected, the densitometry analysis shows that the distribution of Ca^{2+} channel subunits completely overlaps in the graph (Fig. 1*D*), confirming the association of Ca^{2+} channel subunits in a complex.

In a previous study (5), we showed that the γ_2 subunit is part of the Ca^{2+} channel complex as shown in Fig. 1*A*. Recent studies reported that postsynaptic proteins such as AMPA receptor and PSD95 could bind to stargazin when these proteins are expressed in COS7 cells (8–10). Considering these previous studies and our data in Fig. 1, we hypothesized that neuronal Ca^{2+} channels could form a large complex with synaptic proteins in the postsynaptic membrane. To test this hypothesis, we performed a Western blot analysis of the sucrose gradient fractions from rabbit brains with antibodies specifically recognizing subunits of AMPA receptors, GluR1 and GluR2/3, and PSD95. As shown in Fig. 2*A*, GluR1 and GluR2/3 are cosedimented with Ca^{2+} channel subunits. In addition, a fraction of PSD95 cosedimented with Ca^{2+} channel subunits. To clarify the cosedimentation results of AMPA receptors and PSD95, the densitometry analysis was performed with these postsynaptic proteins (Fig. 2*B*). The analysis showed that the distribution of GluR2/3 completely overlaps with Ca^{2+} channel subunits. In the case of PSD95, although the first peak is in the middle of the sucrose gradient, the second peak completely overlaps with Ca^{2+} channel subunits, suggesting partial cosedimentation of PSD95 with Ca^{2+} channels and AMPA receptors (Fig. 2*B*). To confirm that the cosedimentation of the postsynaptic proteins with the Ca^{2+} channel subunits is due to specific interactions with the Ca^{2+} channel complex, sucrose gradient fractions containing both Ca^{2+} channel subunits and synaptic proteins (Fig. 2*A*) were pooled and subjected to immunoprecipitation analyses. Polyclonal anti-α_1 antibodies recognizing $\alpha_1 2.1/2$ subunits of Ca^{2+} channel precipitated both the GluR2/3 and PSD95 (Fig. 2*C*, lane 2). Monoclonal anti-β antibodies recognizing all Ca^{2+} channel β subunits were also able to precipitate these postsynaptic proteins (Fig. 2*C*, lane 3). Furthermore, polyclonal anti-$\gamma_{2/3}$ subunit antibodies precipitated both the GluR2/3 and PSD95 (Fig. 2*C*, lane 4). To rule out the possibility of nonspecific precipitation, the same samples were analyzed with anti-Na^+/K^+ ATPase antibodies. Na^+/K^+ ATPase is abundant in the brain and can be enriched by WGA chromatography. The Na^+/K^+ ATPase was detected in the pooled fraction of the sucrose gradient before immunoprecipitation (Input, Fig. 2C, lane 1), but it was not precipitated by any of the Ca^{2+} channel subunit antibodies (Fig. 2*C*, lanes 2–4). Taken together, these cosedimentation and coimmunoprecipitation results demonstrate a specific association of AMPA receptors and PSD95 with neuronal Ca^{2+} channels in a complex.

Considering that AMPA receptors and PSD95 are major proteins in the PSD, the association of those proteins with Ca^{2+} channels suggests the enrichment of Ca^{2+} channels in the PSD. To examine the possibility, the enrichment of Ca^{2+} channels in the PSD was investigated through subcellular fractionation of synaptic proteins from whole rabbit brain as described in *Methods*. The reliability of our subcellular fractionation was tested through Western blot analyses of the protein samples with antibodies specific for presynaptic or postsynaptic marker proteins (Fig. 3*A*). A presynaptic marker protein, synaptophysin, was highly enriched in both synaptosome and supernatant, which were supposed to include presynaptic proteins extracted by

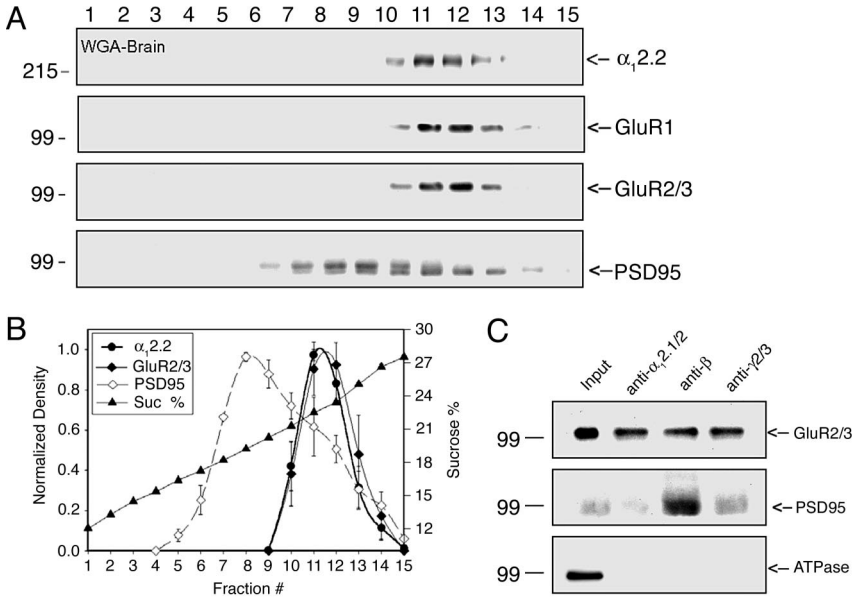

Fig. 2. Association of AMPA receptors and PSD95 with neuronal Ca^{2+} channels. The cosedimentation and coimmunoprecipitation of AMPA receptors and PSD95 with Ca^{2+} channel subunits demonstrate specific association of these proteins in a complex. (*A*) Cosedimentation of AMPA receptor subunits and PSD95 with $\alpha_1$2.2. (*B*) Densitometry of $\alpha_1$2.2, AMPA receptors, and PSD95 from Western blots of sucrose gradient fractions. Fraction #, fraction number of sucrose gradient; Sucrose %, percentage of sucrose. (*C*) Immunoprecipitation of Ca^{2+} channel complexes using three different Ca^{2+} channel subunit antibodies and subsequent immunoblotting for GluR2/3 and PSD95. The first lane (Input) was loaded with the protein aliquots saved before immunoprecipitation. The antibodies used for immunoprecipitation are indicated at the top of each lane: Sheep 37 (anti-$\alpha_1$2.1/2), VD2$_1$ (anti-β), and Rabbit 239 (anti-$\gamma_{2/3}$).

Triton X-100 from the synaptosome. In contrast, postsynaptic marker proteins PSD95 and GluR2/3 were highly enriched in both synaptosome and pellet presumed to include postsynaptic proteins, which were not extracted by Triton X-100 from the synaptosome. These controls demonstrated that presynaptic and postsynaptic proteins were successfully enriched and separated through our subcellular fractionation. The Western blot analyses of the samples with various antibodies specific for Ca^{2+} channel subunits show that all of the subunits are highly enriched in the PSD (Fig. 3 *B* and *C*). This biochemical evidence shows the enrichment of Ca^{2+} channel subunits in the postsynaptic membrane. In addition, as expected, most of the Ca^{2+} channel subunits are also detected in the presynaptic membrane, except $\alpha_1$1.2 (Fig. 3 *B* and *C*). These results indicate that the association of neuronal Ca^{2+} channels with the AMPA receptors and PSD95 is, at least in part, in the PSD.

Having shown that the AMPA receptors could be associated with neuronal Ca^{2+} channels, we next examined whether this association would change Ca^{2+} channel activities using human embryonic kidney (HEK) cells stably expressing $\alpha_1$2.1, $\alpha_2\delta$-1, and β_{1a}, subunits of Ca^{2+} channels (HEK-BI 24-4). Coexpression of AMPA receptors (GluR1+2) does not significantly change the peak current density of the Ca^{2+} channels (Table 1). Peak current densities (pA/pF) were -16.80 ± 2.07 and -17.22 ± 6.61 in Ca_v2.1 and Ca_v2.1 coexpressed with AMPA receptors, respectively (Table 1). Interestingly, the peak currents were observed at different membrane potentials between two groups of cells, suggesting a change in voltage dependence of Ca_v2.1 by AMPA receptor association. The peak currents were observed at 20 mV and 10 mV, in Ca_v2.1 and Ca_v2.1 plus AMPA receptors, respectively. We therefore investigated the voltage-dependent properties of activation of Ca_v2.1. As expected, steady-state activation of Ca_v2.1 is significantly altered by coexpression of AMPA receptors (Fig. 4*A*). There was a significant shift of membrane potential for half-maximal activation ($V_{1/2}$) in Ca_v2.1 by AMPA receptor coexpression (Fig. 4*A* and Table 1). Membrane potential for $V_{1/2}$ was 13.41 ± 2.37 mV ($n = 10$) in cells expressing Ca_v2.1 and significantly shifted to 3.30 ± 1.57 mV

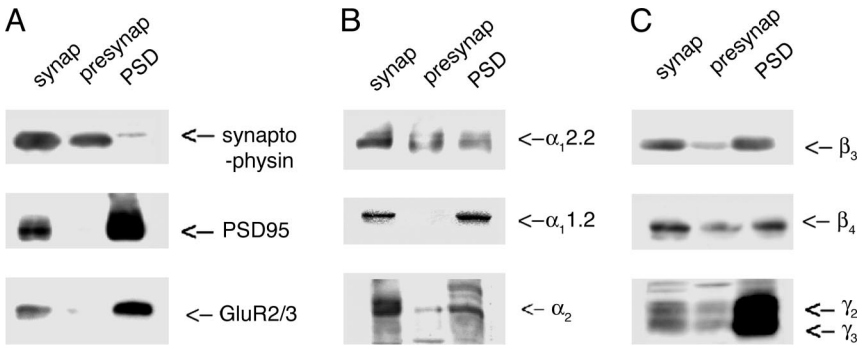

Fig. 3. Subcellular fractionation of rabbit brains. (*A*) Pre- or postsynaptic marker proteins. (*B* and *C*) Ca^{2+} channel subunits. Subcellular fractionation of rabbit brains demonstrates the enrichment of Ca^{2+} channel subunits in the postsynaptic membrane as well as in the presynaptic membrane. The first (synap), second (presynap), and third (PSD) columns were loaded with synaptosomal proteins, presynaptic proteins, and PSD proteins, respectively.

Table 1. Electrophysiological parameters of the $Ca_v2.1$ expressed in HEK cells

Channel	Current density, pA/pF		Capacitance of cell, pF	Steady-state activation parameters from *G-V* curve		Activation kinetics, ms		
	I/C at 10 mV	*I/C* at 20 mV		$V_{1/2}$, mV	*k*, mV	At −10 mV	At 0 mV	At +10 mV
$Ca_v2.1$	−8.21 ± 2.13	−16.80 ± 2.07	20.26 ± 1.92	13.41 ± 2.37	−4.58 ± 0.65	242.66 ± 26.39	117.34 ± 26.28	36.56 ± 3.90
$Ca_v2.1$ + AMPAR	−17.22 ± 6.61*	−13.46 ± 3.10	22.79 ± 2.26	3.30 ± 1.57**	−2.64 ± 0.64*	124.09 ± 27.91**	62.63 ± 14.32*	32.30 ± 2.57

Ten cells were used for each experiment. Values are presented as mean ± SEM. *, $P < 0.05$; **, $P < 0.01$. (with respect to $Ca_v2.1$). AMPAR, AMPA receptor; *I*, current; *C*, capacitance; *G*, conductance; *V*, potential; $V_{1/2}$, membrane potential for half-maximal activation; *k*, slope factor.

($n = 10$) upon coexpression of AMPA receptors ($P < 0.001$). The slope factor (k) of the activation curve for $Ca_v2.1$ was also significantly affected by AMPA receptor coexpression (Fig. 4*A* and Table 1). In addition, the properties of voltage-dependent inactivation were studied. However, AMPA receptor coexpression does not significantly affect either the membrane potential for half-maximal inactivation or the slope factor of the steady-state inactivation of the $Ca_v2.1$ currents (data not shown).

Activation kinetics of $Ca_v2.1$ and $Ca_v2.1$ plus AMPA receptor were also compared by analyzing the time-to-peak (TP) of $Ca_v2.1$ currents in a series of test potentials ranging from −10 to +50 mV. As illustrated in Fig. 4*B*, the activation of currents is significantly accelerated by AMPA receptor coexpression at the membrane potentials −10 and 0 mV (see also Table 1). For example, at −10 mV, TP values were 242.66 ± 26.39 ms ($n = 10$) and 124.09 ± 27.91 ms ($n = 10$) in $Ca_v2.1$ and $Ca_v2.1$ coexpressed with AMPA receptors, respectively ($P < 0.01$). In addition, the properties of inactivation kinetics were studied. However, inactivation kinetics of $Ca_v2.1$ are not significantly affected by coexpression of AMPA receptors (data not shown).

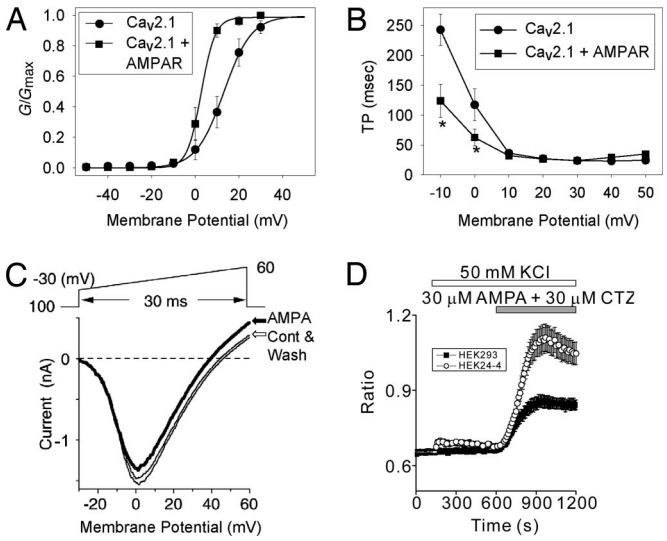

Fig. 4. Functional coupling between $Ca_v2.1$ and AMPA receptors. The activity of heterologously expressed $Ca_v2.1$ or AMPA receptors was analyzed by using HEK or HEK-BI 24-4 cells. The activities of $Ca_v2.1$ or AMPA receptors were significantly altered by the coexpression of the two receptors. (*A*) Superimposed plots of steady-state activation (G/G_{max}) curves of $Ca_v2.1$. (*B*) Superimposed plots of $Ca_v2.1$ activation kinetics (TP, time-to-peak). *, statistically significant difference in certain value between two groups. Electrodes were filled with internal solution containing 155 mM CsCl, 11 mM EGTA, 0.3 mM Li-GTP, 4 mM Mg-ATP, and 10 mM Hepes (pH 7.4 with CsOH). The recording chamber was filled with external solution containing 10 mM $CaCl_2$, 125 mM tetraethylammonium chloride (TEA-Cl), 10 mM Hepes, and 5 mM glucose. The external solution was adjusted to pH 7.3 with CsOH and to 297 mosmol/liter with sucrose. Test potentials were applied for 350 ms from a holding potential of −90 mV. (*C*) Current–voltage relationship of $Ca_v2.1$ coexpressed with AMPA receptors with (AMPA, bold line) or without AMPA treatment. The normal pipette solution contained 85 mM Cs-aspartate, 40 mM CsCl, 2 mM $MgCl_2$, 5 mM EGTA, 2 mM Na_2ATP, 5 mM Hepes, and 8 mM creatinine-phosphate (pH adjusted to 7.2 with CsOH). The external solution for recording of Ca^{2+} channel current contained 3 mM $BaCl_2$, 150 mM TEA-Cl, 10 mM Hepes, and 10 mM glucose (pH adjusted to 7.4 with TEA-OH). (*D*) Ca^{2+} response induced by AMPA (30 μM) and the AMPA receptor-specific modulator cyclothiazide (CTZ, 30 μM) HEK cells expressing GluR1 alone (HEK 293) or GluR1 plus $Ca_v2.1$ (HEK24-4) after 8 min exposure to high K^+ (50 mM) solution. The ''Ratio'' was obtained by exciting fura-2 alternately at 340 and 380 nm.

Having shown that the none-active AMPA receptors could modulate $Ca_v2.1$, we next examined whether $Ca_v2.1$ current could be modulate by stimulation of the AMPA receptor using the HEK-BI 24-4 cells. A 30-ms positive ramp protocol from −30 to 60 mV was applied at 1/15 Hz interval in the external solution containing 3 mM Ba^{2+} as a charge carrier (Fig. 4*C*). The Ba^{2+} current was increased by membrane depolarization above −30 mV, and increasingly reached the maximum around 2 mV. The apparent reversal potential was 45 mV. AMPA (100 μM) reduced the peak current amplitude to 88 ± 2% ($n = 7$) of the control Ba^{2+} current after a 2.5-min application (bold trace in Fig. 4*C*). Threshold and the membrane potential giving the maximum current amplitude were unaffected, whereas the reversal potential was slightly shifted in the hyperpolarizing direction by 5 mV. The current suppression was slowly and partially reversed by wash (1.5 min). We finally confirmed the functional expression of AMPA receptors by exchanging the external solution to the tyrode and applying 100 μM AMPA and 50 μM cyclothiazide (CTZ): the drugs slowly developed typical GluR1+2 inward currents at a holding potential of −70 mV (data not shown). Because AMPA receptors are rapidly desensitized by AMPA in the absence of CTZ and external solution contained Ba^{2+} and tetraethylammonium $(TEA)^+$, contribution of AMPA currents should be very little or not at all during the observed change of Ba^{2+} currents by AMPA, leading to an idea that stimulation of GluR1+2 by AMPA elicits current-independent suppression of $Ca_V2.1$ channels.

We also investigated whether Ca^{2+} channel association could modulate AMPA receptor activities using the HEK-BI 24-4 cells. Interestingly, coexpression of $Ca_v2.1$ with AMPA receptors does change the Ca^{2+} influx through the AMPA receptors that consist of GluR1 subunits (Fig. 4*D*). In depolarizing high K^+ solution, AMPA-induced Ca^{2+} entry through the AMPA receptors was increased about twice in the HEK-B2 24-4 cells coexpressing $Ca_v2.1$ compared with that in the HEK cell expressing GluR1 alone.

Discussion

There have been several electrophysiological and immunocytochemical studies demonstrating the expression of voltage-activated Ca^{2+} channel in the postsynaptic membrane (13–17). However, there has been no biochemical study showing the enrichment of the channel in the postsynaptic membrane. In the present study, we show not only the enrichment of Ca^{2+} channels in the postsynaptic membrane but also the association of postsynaptic proteins with the Ca^{2+} channels in native brain tissue through a series of biochemical studies. Furthermore, our electrophysiological and Ca^{2+} imaging studies using heterologously

expressed neuronal Ca^{2+} channels and AMPA receptors demonstrate functional association of these two proteins.

A previous electrophysiological study of the postsynaptic Ca^{2+} channel suggested that the major Ca^{2+} channel currents expressed in the dendrite of hippocampal neurons are $Ca_v2.1$ and $Ca_v2.2$ currents (17). Based on this finding, our biochemical analysis of postsynaptic Ca^{2+} channels was focused on $Ca_v2.1$ and $Ca_v2.2$. Because $\alpha_1 2.1$ showed multiple bands, possibly consisting of splice variants as reported (18), all of our sucrose gradient fractionation data were presented with $\alpha_1 2.2$ signals, although both proteins were always analyzed simultaneously. In addition, we did not investigate the association of AMPA receptors and PSD95 with $Ca_v1.2$ because a recent study (19) suggested that the postsynaptic proteins are not associated with $Ca_v1.2$.

Our studies showing the association of AMPA receptors and Ca^{2+} channels in the postsynaptic membrane raise a very interesting question: What is the physiological meaning of the Ca^{2+} channel association with AMPA receptors? It is well known that an increase in postsynaptic $[Ca^{2+}]_i$ is an important factor for synaptic plasticity, such as LTP and long-term depression (LTD) (20). The trafficking of AMPA receptors has also been suggested as one of the key mechanisms for LTP and LTD (1). Considering the roles of $[Ca^{2+}]_i$ and AMPA receptor trafficking in synaptic plasticity, the assembly of AMPA receptors and Ca^{2+} channels may be important for the regulation of AMPA receptor trafficking. In fact, a recent study (21) demonstrated that the change of local $[Ca^{2+}]_i$ could regulate the lateral movement of AMPA receptors in cultured hippocampal neurons. Considering these studies, our electrophysiological analysis of the association between Ca^{2+} channels and AMPA receptors not only confirms their physical association but also suggests some clues about the possible function of their association. By coexpression of AMPA receptors, the steady-state activation curve of $Ca_v2.1$ was shifted to negative membrane potential, and activation was accelerated at membrane potentials more negative than that of peak current of $Ca_v2.1$ (Fig. 4 *A* and *B* and Table 1). This finding means that association of AMPA receptors with Ca^{2+} channels could increase the activity of Ca^{2+} channels at a lower membrane potential than that of peak current. In a real physiological situation, the functional association could cause more activation of Ca^{2+} channels with a relatively small change of membrane potential in a neuron. The increase of $Ca_v2.1$ activity could increase the Ca^{2+} influx, resulting in a favorable local environment for the stabilization of AMPA receptors in synapse. On the other hand, when the AMPA receptors are activated, the association of AMPA receptor negatively modulated the current of $Ca_v2.1$ (Fig. 4*C*). The decrease of Ca^{2+} channel activity could decrease the Ca^{2+} influx, resulting in a favorable local environment for the lateral movement of AMPA receptors. In that way, the assembly of AMPA receptor and Ca^{2+} channel could be an important part in the molecular mechanism underlying synaptic plasticity. It has been suggested that the change of $[Ca^{2+}]_i$ in local environment regulates the binding of chaperone proteins to AMPA receptors or phosphorylation of AMPA receptors (1). Based on recent studies (5, 8, 22–24) and biochemical data in this study (Fig. 2), PSD95 or Ca^{2+} channel γ_2 subunits (stargazin) could be a candidate chaperon protein modulating AMPA receptor trafficking depending on the Ca^{2+} influx through Ca^{2+} channels.

Methods

Partial Purification of Native Ca^{2+} Channel Complexes. The Ca^{2+} channel complex was partially purified from skeletal muscles or brains of rabbits as described (5). Briefly, from 50 mg of microsomes washed with 2 M KCl twice, the Ca^{2+} channel complexes were extracted with 1% digitonin (Biochemica & Synthetica, Staad, Switzerland). Unless otherwise indicated, the Ca^{2+} channel complexes were then enriched through WGA chromatography and sucrose density gradient.

Immunoprecipitation of Ca^{2+} Channel Subunits. Ca^{2+} channel subunits and postsynaptic proteins were immunoprecipitated from the partially purified Ca^{2+} channel complex as described without major modification (5).

Densitometry Analysis of Protein Signals from Western Blots. Protein signals in Western blots were developed by enhanced chemiluminescence (ECL) (SuperSignal or DuraSignal; Pierce) and imaged by using an image capturing system (MultiImage; Alpha Innotech, San Leandro, CA). The density of protein signals was measured by using the image process program Fluorchem 3.04A (Alpha Innotech) just under the saturation of the strongest signal. The density of each protein was normalized through the measurements of approximately five to six independent experiments. After statistical analysis, the mean ± SEM values were plotted as a function of fraction number of sucrose gradient, and the sucrose percentage was measured with a refractometer (Milton Ray, Rochester, NY).

Subcellular Fractionation. To purify presynaptic and postsynaptic proteins, subcellular fractionation was performed based on a previously described method (25), with some modification. Whole rabbit brains (17 g) were homogenized in a homogenization buffer containing 4 mM Hepes (pH 7.4), 320 mM sucrose, 5 mM EDTA, 5 mM EGTA, and a mixture of protease inhibitors. Cell debris and nuclei were removed by centrifugation at 800 × *g* for 10 min. The supernatant was centrifuged at 9,000 × *g* for 15 min to obtain crude synaptosomal fraction as pellet. The crude synaptosomes were resuspended in the homogenization buffer and centrifuged at 10,000 × *g* for 15 min. The washed crude synaptosomes were lysed by hypoosmotic shock in water, rapidly adjusted to 1 mM Hepes/NaOH (pH 7.4), and stirred on ice for 30 min. After centrifugation of the lysate at 25,000 × *g* for 20 min, the pellet was resuspended in 0.25 M buffered sucrose. The synaptosome membranes were then further enriched through a discontinuous sucrose gradient containing 0.8/1.0/1.2 M sucrose. After centrifugation at 65,000 × *g* for 2 h, the synaptosomal plasma membranes (SPM) were collected from 1.0/1.2 M sucrose interface. Presynaptic membrane proteins were extracted from the SPM through solubilization with 0.2% Triton X-100 in 0.5 mM Hepes/NaOH (pH 7.4), followed by centrifugation at 65,000 × *g* for 20 min. The resulting supernatant and pellet were designated as presynaptic and PSD fractions, respectively.

Antibodies and Western Blot Analysis. Polyclonal antibodies Sheep 37, Sheep 46, Sheep 49, Rabbit 145, and Rabbit 239, specific for the neuronal Ca^{2+} channel subunits $\alpha_1 2.1/2$, $\alpha_1 2.2$, β_3, β_4, and $\gamma_{2/3}$, respectively, have been described (6, 26–28). Antibodies IIID5E1, Guinea Pig 1, Sheep 6, and Guinea Pig 16, specific for the skeletal muscle Ca^{2+} channel subunits $\alpha_1 1.1$, $\alpha_2\delta$, β_{1a}, and γ_1, respectively, have been characterized (7, 29–31). Monoclonal antibody $VD2_1$, which recognizes all Ca^{2+} channel β subunits, has been described (32). Anti-GluR2/3 serum was a gift from M. Sheng. The antibodies specific for GluR1 (Sigma), Na^+/K^+ ATPase (Affinity BioReagents, Golden, CO), $Ca_v\,\alpha_1 2.1$ subunit (Alomone, Jerusalem), and $Ca_v\,\alpha_2\delta$-1 (Alomone) were obtained from commercial sources as indicated. Western blot analysis was performed as described (5).

Cell Culture and Transfection. The HEK-BI 24-4 cell line stably expressing the $\alpha_1 2.1$, $\alpha_2\delta$-1, and β_{1b} subunits of Ca^{2+} channels was established and maintained as described (6). Transient transfections of GluR1 and/or GluR2 were performed by using FuGENE 6 (Roche Molecular Systems, Indianapolis) or SuperFect Transfection Reagent (Qiagen, Valencia, CA) according to

the manufacturer's protocol. cDNA clones used for the transfection were as follows: Rat GluR1 in pRK5 and Rat GluR2 in pRK5. In addition, plasmids encoding the eGFP (BD Biosciences Clontech) or pGFP-F (Clontech) were cotransfected with the other cDNAs to select positively transfected cells. Furthermore, the protein expressions of the transfected genes were confirmed through Western blot analyses with specific antibodies for each protein.

Electrophysiological Recording and Analysis. Ca^{2+} channel activity was recorded from the HEK-BI 24-4 cells by using the whole-cell patch-clamp technique (33) at room temperature. Pipette resistance ranged from 2 to 4 MΩ when filled with the pipette solutions. Output signals were filtered at 2 kHz and sampled at 10 kHz. Steady-state activation curves were described by a modified Boltzmann equation: $G = G_{max}/[1 + \exp((V_m - V_{1/2})/k)]$. G represents conductance obtained from the equation: $G = I/(V_m - E)$. I represents current density, G_{max} is maximum conductance, V_m is test potential, E is reversal potential, $V_{1/2}$ is potential of half-activation, and k is slope factor. To obtain the estimates of the activation rates, time-to-peak was measured by using an analytical routine of pClamp 8.1 program. The tyrode solution contained 150 mM NaCl, 5 mM KCl, 2 mM $CaCl_2$, 1 mM $MgCl_2$, 10 mM Hepes, and 10 mM glucose (pH adjusted to 7.4 with NaOH).

Fluorescent Measurements. Fluorescence images of the cells were recorded and analyzed with a video images analysis system (ARGUS-20/CA; Hamamatsu Photonics, Hamamatsu City, Japan). The fura-2 fluorescence at an emission wavelength of 510 nm (bandwidth, 20 nm) was obtained at room temperature by exciting fura-2 alternately at 340 and 380 nm (bandwidth, 11 nm). The 340:380 nm ratio images were obtained on a pixel-by-pixel basis. The fura-2 fluorescence was measured in Hepes-buffered saline (HBS) containing 107 mM NaCl, 6 mM KCl, 1.2 mM $MgSO_4$, 2 mM $CaCl_2$, 11.5 mM glucose, and 20 mM Hepes (adjusted to pH 7.4 with NaOH).

We thank Drs. R. L. Huganir (The Johns Hopkins University Medical School, Baltimore) and M. Sheng (Massachusetts Institute of Technology, Cambridge, MA) for their kind gifts of GluR cDNAs and anti-GluR2/3 antibody, respectively. We thank the University of Iowa Diabetes and Endocrinology Research Center (National Institutes of Health Grant DK25295). M.-G.K. was partly funded by an Epilepsy Foundation Predoctoral Fellowship. K.P.C. is an Investigator of the Howard Hughes Medical Institute.

1. Song, I. & Huganir, R. L. (2002) *Trends Neurosci*. **25,** 578–588.
2. Kapur, A., Yeckel, M. F., Gray, R. & Johnston D. (1998) *J. Neurophysiol*. **79,** 2181–2190.
3. Kovalchuk, Y., Hanse, E., Kafitz, K. W. & Konnerth, A. (2002) *Science* **295,** 1729–1734.
4. Witcher, D. R., De Waard, M., Kahl, S.D. & Campbell, K.P. (1994) *Methods Enzymol*. **238,** 335–348.
5. Kang, M. G., Chen, C. C., Felix, R., Letts, V. A., Frankel, W. N., Mori, Y. & Campbell, K. P. (2001) *J. Biol. Chem*. **276,** 32917–32924.
6. Letts, V. A., Felix, R., Biddlecome, G. H., Arikkath, J., Mahaffey, C. L., Valenzuela, A., Bartlett, F. S., II, Mori, Y., Campbell, K. P. & Frankel, W. N. (1998) *Nat. Genet*. **19,** 340–347.
7. Sharp, A. H. & Campbell, K. P. (1989) *J. Biol. Chem*. **264,** 2816–2825.
8. Chen, L., Chetkovich, D. M., Petralia, R. S., Sweeney, N. T., Kawasaki, Y., Wenthold, R. J., Bredt, D. S. & Nicoll, R. A. (2000) *Nature* **408,** 936–943.
9. Tomita, S., Adesnik, H., Sekiguchi, M., Zhang, W., Wada, K., Howe, J. R., Nicoll, R. A. & Bredt, D. S. (2005) *Nature* **435,** 1052–1058.
10. Chetkovich, D. M., Chen, L., Stocker, T. J., Nicoll, R. A. & Bredt, D. S. (2002) *J. Neurosci*. **22,** 5791–5796.
11. Tomita, S., Chen, L., Kawasaki, Y., Petralia, R. S., Wenthold, R. J., Nicoll, R. A. & Bredt, D. S. (2003) *J. Cell Biol*. **26,** 805–816.
12. Price, M. G., Davis, C. F., Deng, F. & Burgess, D. L. (2005) *J. Biol. Chem*. **280,** 19711–19720.
13. Tank, D. W., Sugimori, M., Connor, J. A. & Llinas, R. R. (1988) *Science* **242,** 773–777.
14. De Schutter, E. & Bower, J. M. (1994) *Proc. Natl. Acad. Sci. USA* **91,** 4736–4740.
15. Kulik, A., Nakadate, K., Hagiwara, A., Fukazawa, Y., Lujan, R., Saito, H., Suzuki, N., Futatsugi, A., Mikoshiba, K., Frotscher, M., *et al.* (2004) *Eur. J. Neurosci*. **19,** 2169–2178.
16. Miyazaki, T., Hashimoto, K., Shin, H. S., Kano, M. & Watanabe, M. (2004) *J. Neurosci*. **24,** 1734–1743.
17. Kavalali, E. T., Zhuo, M., Bito, H. & Tsien, R. W. (1997) *Neuron* **18,** 651–663.
18. Scott, V. E., Felix, R., Arikkath, J. & Campbell, K. P. (1998) *J. Neurosci*. **18,** 641–647.
19. Davare, M. A., Avdonin, V., Hall, D. D., Peden, E. M., Burette, A., Weinberg, R. J., Horne, M. C., Hoshi, T. & Hell, J. W. (2001) *Science* **293,** 98–101.
20. Zucker, R. S. (1999) *Curr. Opin. Neurobiol*. **9,** 305–313.
21. Borgdorff, A. J. & Choquet, D. (2002) *Nature* **417,** 649–653.
22. Schnell, E. Sizemore, M., Karimzadegan, S., Chen, L., Bredt, D. S. & Nicoll, R. A. (2002) *Proc. Natl. Acad. Sci. USA* **99,** 13902–13907.
23. Moss, F. J., Viard, P., Davies, A., Bertaso, F., Page, K. M., Graham, A., Canti, C., Plumpton, M., Plumpton, C., Clare, J. J., *et al.* (2002) *EMBO J*. **21,** 1514–1523.
24. Zhang, Y., Mori, M., Burgess, D. L. & Noebels, J. L. (2002) *J. Neurosci*. **22,** 6362–6371.
25. Huang, Y. Z., Wang, Q., Xiong, W. C. & Mei, L. (2001) *J. Biol. Chem*. **276,** 19318–19326.
26. Witcher, D. R., De Waard, M. & Campbell, K. P. (1993) *Neuropharmacology* **32,** 1127–1139.
27. Witcher, D. R., De Waard, M., Sakamoto, J., Franzini-Armstrong, C., Pragnell, M., Kahl, S. D. & Campbell, K. P. (1993) *Science* **261,** 486–489.
28. Liu, J. De Waard, M., Scott, V. E. S., Gurnett, C. A., Lennon, V. A. & Campbell, K. P. (1996) *J. Biol. Chem*. **271,** 13804–13810.
29. Ahern, C. A., Powers, P. A., Biddlecome, G. H., Roethe, L., Vallejo, P., Mortenson, L., Strube, C., Campbell, K. P., Coronado, R. & Gregg, R. G. (2001) *BMC Physiol*. **1,** 8.
30. Leung, A. T., Imagawa, T. & Campbell, K. P. (1987) *J. Biol. Chem*. **262,** 7943–7946.
31. Pragnell, M., Sakamoto, J., Jay, S. D. & Campbell, K. P. (1991) *FEBS Lett*. **291,** 253–258.
32. Sakamoto, J. & Campbell, K. P. (1991) *J. Biol. Chem*. **266,** 18914–18919.
33. Hamill, O. P., Marty, A., Neher, E., Sakmann, B. & Sigworth, F. J. (1981) *Pflügers Arch*. **391,** 85–100.